Journal of Applied Polymer Science

Self-assembly of Bovine Serum Albumin and Poly(Acrylic Acid) Induced by Noncovalent Bonds

Weiping Du,[1,2] Yansong Wang[1]

[1]State Key Laboratory for Modification of Chemical Fibers and Polymer Materials, College of Material Science and Engineering, Dong Hua University, Shanghai 201620, People's Republic of China

[2]Reference & Consulting Department, Library, Dong Hua University, Shanghai 201620, People's Republic of China

Correspondence to: W. Du (E-mail: h-wp@163.com)

ABSTRACT: Bovine serum albumin/poly(acrylic acid), BSA/PAA, nano-scaled particles were produced by noncovalent bonds induced self-assembly method at acid pH area. Proper conditions during preparation process, such as pH value, BSA/PAA weight ratio(WR), PAA molecular weight, were researched by studying the hydrodynamic diameter, polydispersity index, and ζ potential of the nanoparticles. Complex formation between BSA and PAA was studied by FT-IR, AFM, and TEM. BSA chains are supposed to be partly trapped in the nanoparticles core after interaction with PAA because of the electrostatic attractions and hydrogen bonds interactions between BSA and PAA, while the rest of the BSA chains should form the shell of the nanoparticles. © 2012 Wiley Periodicals, Inc. J. Appl. Polym. Sci. 000: 000–000, 2012

KEYWORDS: BSA; polyelectrolytes; self-assembly; biopolymers; noncovalent bonds

Received 3 May 2011; accepted 6 May 2012; published online
DOI: 10.1002/app.38038

INTRODUCTION

Bioconjugations of synthetic polyelectrolytes (PE) with biomacromolecules, such as protein, have attracted much attention in the last decades for its great advantages in biomedicine field.[1–15] Synthetic polyelectrolytes could induce a variety of biological activities, especially in the immunological research.[16–18] Using polyanions as protein carriers to resist viruses exhibit great immunoadjuvant activity, which was superior to inoculation method. For example, the primary antibody response to sheep erythrocytes has been enhanced using polyanions.[19–21] Among various polyanions, PAA appears much higher antiviral activity and less cytotoxic than others (e.g. dextran sulfate, polystyrensulfonate, and polyvinylsulfate). Bovine serum albumin (BSA) is a globular protein and possesses about 583 amino acids with 17 disulfide bonds and one free cysteine group in its native state.[22–24] It has relatively high water solubility because of its large number of ionizable amino acids.[25] BSA can bind many different types of amphiphilic biological molecules, which are believed to play an important role in determining the physiological function.[26]

Biomacromolecules/PE complexes could be formed as a result of the reaction between the polyion chains and the oppositely charged groups of the protein molecule. The use of PAA as a carrier for model protein antigens, such as bovine serum albumin or ovalbumin, with the components linked by covalent bonds, has made it possible to stimulate the production of protein-specific antibodies.[21] In those cases, polyelectrolyte macromolecules do not contain the corresponding functional groups for binding. So, it is necessary to modify the carrier polymer to change its effect upon biological systems.[27,28] Self-assembly of component polymers via specific interactions to construct noncovalent connected micelles (NCCM) was first proposed by Jiang.[29] Recently, several investigators utilized the behavior of linear synthetic polyelectrolytes metal ions as complex stabler, locating at the interface between two polymers. Insoluble complexes of BSA with nonfractionated PAA in the presence of Ba^{2+} have been described by Morawetz et al.[30] Mustafaev et al. have studied the Cu^{2+}-induced interaction between BSA and PAA.[27,28] The formation of these complexes involves the use of low concentrations of Cu^{2+} ions, which promote the binding of water-borne poly(*N*-isopropylacrylamide-*co*-acrylic acid) to BSA.[31–34] The release behavior for drugs of BSA/PAA has also been researched.[35–37]

In this work, the self-assembly of BSA/PAA via noncovalent bonds, including the electrostatic attractions and H-bonding interactions, to fabricate NCCM in the acid stage was proposed. Self-assemble BSA/PAA nanoparticles are pH-responsible due to the pH-sensibility of the compounds. Proper conditions during preparation process, such as pH value, BSA/PAA weight ratio

(WR), PAA molecular weight, were researched. A probable reaction mechanism was proposed, too.

EXPERIMENTAL

BSA and PAA with different molecular weight purchased from Sigma were used without further purification. According to a certain BSA/PAA weight ratio, PAA aqueous solution (0.125% w/w) was added into 0.125% BSA solution at pH = 2.6 under gradual agitation, then the mixture solution was stirred slowly at room temperature for 15 min. The pH values of the mixture were adjusted by adding dilute NaOH or HCl (Shanghai Chemical) (1 mol/mL) aqueous solutions. Then the reaction mixture was dialyzed against the aqueous solution (pH = 2.6) for 2 days to remove unreacted materials and dissociative PAA oligomers. Hydrodynamic diameter ($<D_h>$), polydispersity index (PDI), and ζ potential of the nanoparticles were determined using Malvern DTS1060 at 25°C. The results were averaged on five times of measurements. Infrared absorption spectrum of drying PAA, BSA, BSA/PAA polymer nanoparticles were studied by FT-IR (Nicolet Magna 550 spectrometer, Nicolet). The changes of transparency of BSA/PAA solutions with a weight ratio of 4.0 were recorded at 450 nm on a spectrophotometer (Lambda 35 UV-Vis Spectrometer, Perkin-Elmer) in various pH values at 25°C. A Nanoscope IV (Digital Instruments) atomic force microscope (AFM) in tapping mode was used to study the surface morphology of the nanoparticles. One drop of properly diluted nanoparticle dispersion was placed on freshly cleaved mica substrate and dried at room temperature. TEM observations were conducted on a Philips CM 120 electron microscope at an accelerating voltage of 80 kV. The samples with BSA/PAA weight ratio 4 and pH 2.6 were prepared by dropping nanoparticles solutions onto copper grids and dried naturally.

RESULTS AND DISCUSSION

ξ Potentials of BSA Solution and BSA/PAA Nanoparticle upon pH Change

The structure of BSA could change easily due to its pH dependence,[16,17] for which it was usually used as a good template for conformational study. The ξ potentials of BSA solution and BSA/PAA nanoparticles at various pH values were studied, as seen in Figure 1. The relatively large absolute value of ξ potential means the surface charge of the nanoparticles is high. The particle aggregation is difficult due to the repulsive force between the nanoparticles, which contributes to improve the stability. It can be seen that the ξ potentials that express the surface charges of nanoparticles reach the maximum around pH 2.5 both for BSA solution and BSA/PAA nanoparticle. BSA undergoes reversible conformational isomerization in the pH range adopted. When pH changes from 1.45 to 2.5, helix content in BSA conformation reaches to minimum. The expanded BSA association as well as the intense ionization occurred in this pH range results in high ξ potential value. In addition, due to serious charge shielding effect in low pH value region, ξ potential increases with enhanced pH value, resulting in ξ maximum at pH 2.5. Then with pH value increasing to 4.8, helix content in BSA rises and reaches to the maximum, 55%, which induces the conformations shrink into a cordate structure. At this time, solubility of BSA solution arrives to the lowest value and the isoelectric point, 4.8, which is consistent with literatures,[38] appears. With further increasing of pH, BSA helix content reduces again and the ionization of carboxylic acid groups in the aminophenol of BSA increases which results in the negative value of ξ.

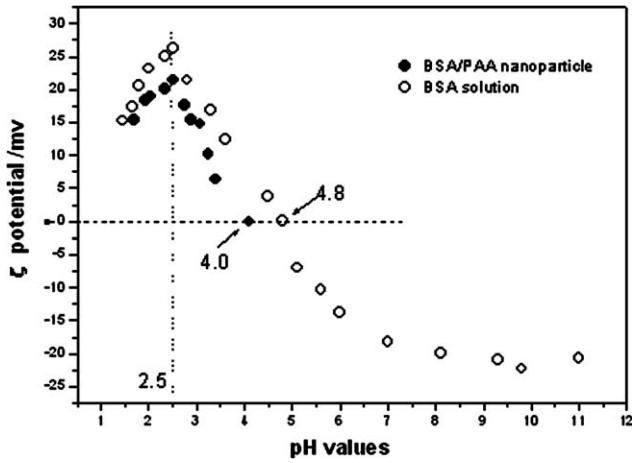

Figure 1. The ξ potentials of 1 mg/mL BSA as well as 1 mg/mL BSA/PAA nanoparticle (weight ratio of BSA/PAA = 4.0) as a function of pH values.

ξ potentials of BSA/PAA nanoparticle were measured at a pH range of 1.7−4.0 (Figure 1). ξ potential, which is directly related to the surface charge on the nanoparticles, is an index expressing electrostatic interaction between BSA and PAA. PAA is a polyanion with a pK_a of 4.7. While carboxyl groups ionized partly at pH 2.5−4.7, the degree of ionization increases in this pH range. As seen in Figure 1, from pH 1.7 to 2.5, the increase in ξ potential mostly happens as a result of serious charge shielding effect, in which H-bonding interaction in BSA/PAA nanoparticles is remarkable. While for pH 2.5−4.0, electrostatic attraction is dominant between opposite charges in BSA and PAA. The nanoparticles' ξ potential reaches minimums at pH 4.0, indicating the ionization of carboxyl groups in PAA and BSA, which neutralizes all the positive charges in BSA. At pH > 4.0, BSA/PAA nanoparticles could not exist stably.

$<D_h>$ of BSA/PAA Nanoparticles

The effective BSA/PAA self-assembly occurred at the pH range from 1.7 to 3.5, detected by DLS measurement, as shown in Figure 2. Large $<D_h>$ will increase the possibility of particle precipitation, thus the particle stability decreases. From pH 1.7 to 2.4, the average size of the nanoparticle decreases dramatically, and the electrostatic attractive between BSA and PAA is not strong enough due to shielding effect in low pH value. Relative uniform size nanoparticles can be fabricated at pH 2.4−3.1 with small size of about 150 nm. Further increasing the environmental pH value leads to linear decrease in ξ potential of nanoparticles because of the aggregation between the particles. Thus, the suitable self-assembly pH for BSA/PAA nanoparticles is around pH 2.4 to 3.1.

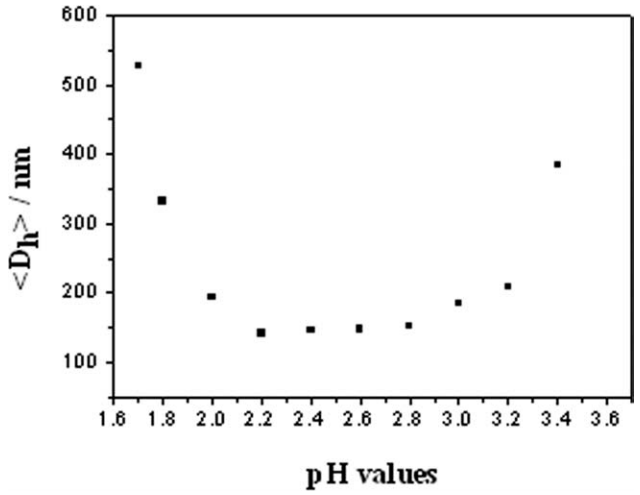

Figure 2. The $<D_h>$ of BSA/PAA nanoparticles as a function of pH values (BSA/PAA = 4.0, [BSA] = 1 mg/mL).

Effect of PAA Molecular Weight on the Self-Assemble of BSA/PAA Nanoparticle

The effect of PAA molecular weight on the self-assemble of BSA/PAA nanoparticle was studied. Figure 3 expresses the $<D_h>$ of BSA/PAA nanoparticle with various PAA molecular weights. There exist small $<D_h>$ nanoparticles in low PAA molecular weight region, which is not stable enough until PAA molecular weight reaches 15K because there is a double peak in the hydrodynamic diameter distribution curves tested by DTS1060. When PAA molecular weight is over 15 kDa, the comparable uniform nanoparticles $<D_h>$ could be obtained, forming compacted nanoparticles. With further increase of PAA molecular weight to 40 kDa, the $<D_h>$ of BSA/PAA nanoparticles decreases linearly. This is because the hydrophobic action of the particles increases, which favors the stability of the nanoparticles. $<D_h>$ increase for PAA molecular weight from 40 to 60 kDa is because excessive hydrophobic interactions in nanoparticles lead to aggregation and deposition.

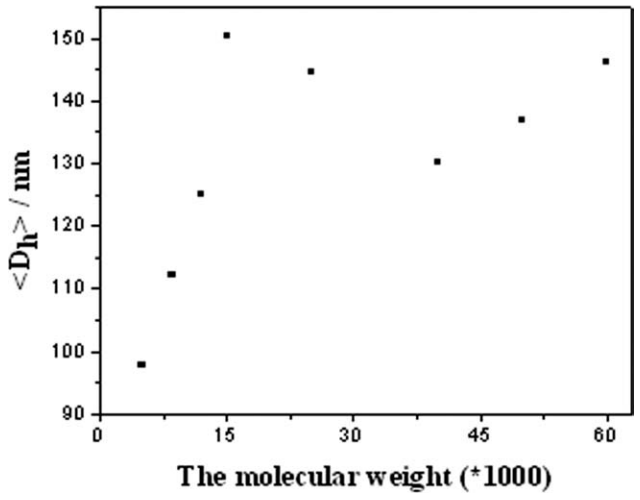

Figure 3. The $<D_h>$ of BSA/PAA nanoparticle as a function of the PAA molecular weight (BSA/PAA = 4.0, [BSA] = 1 mg/mL, pH = 2.6).

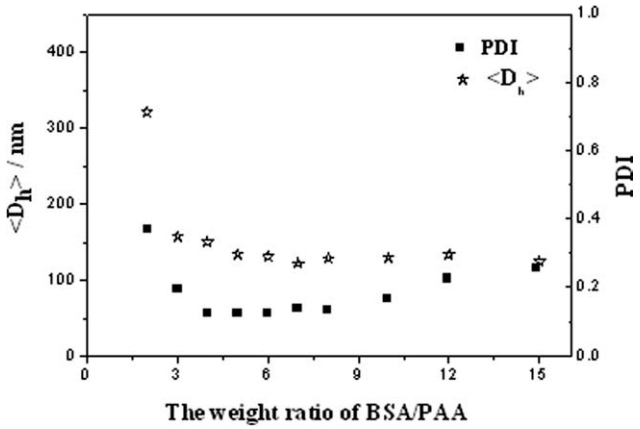

Figure 4. $<D_h>$ and PDI as function of the weight ratio of BSA /PAA ([BSA] = 1 mg/mL, pH = 2.6).

Effect of BSA/PAA Weight Ratio on the Self-Assemble

The weight ratio of BSA/PAA in preparation process is a primary factor on the nanoparticle's stability and structure. Figure 4 shows $<D_h>$ and PDI of the nanoparticles with various weight ratio of BSA/PAA. When BSA content is very small, the incompacted nanoparticles were obtained due to weak interaction between BSA and PAA. The charges in carboxyl groups of PAA neutralize most positive charges in BSA, reducing the stability of the nanoparticles. Even when WR of BSA/PAA reaches 2, the nanoparticles cannot disperse well in the solution, which leads to higher distribution. While the $<D_h>$ of nanoparticles decreases when WR rises, indicating a much more compactable structures of the nanoparticles achieved, and the nanoparticles' size distribution, PDI value, decreases for the same reason. The appropriate ratio of BSA/PAA is 3 $\sim$ 8, in view of Figure 4.

The ζ potentials of nanoparticles with various BSA/PAA ratios were also detected to further study the stabilities and superficial charges of nanoparticles, as seen in Figure 5. The carboxyl

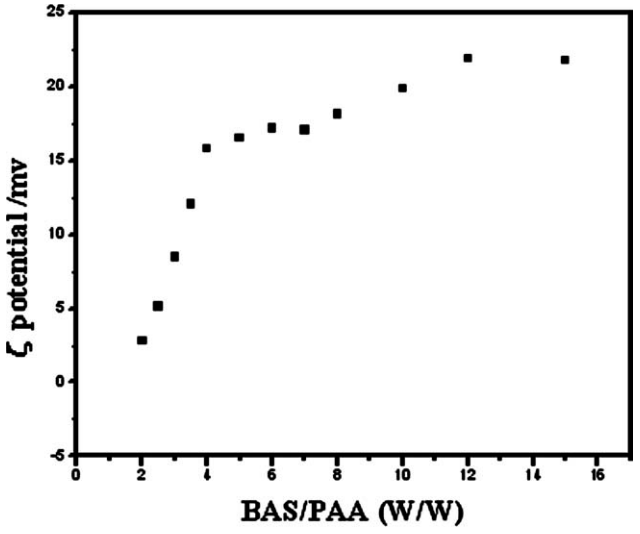

Figure 5. ζ potentials of nanoparticles as a function of the weight ratio of BSA/PAA ([BSA] = 1 mg/mL, pH = 2.6).

groups of PAA and BSA are electronegative, while amido groups of BSA are electropositive. When self-assembly occurs due to electrostatic attraction, the charge density of BSA decreases at the same time, which results in low ζ potential and low stabilization. Only when weight ratio of BSA/PAA is over 3, the ζ potentials of nanoparticles come to a relative high value, indicating comparative stable structure is obtained.

The Interaction Between BSA and PAA Tested by FTIR Method

To illustrate the interactions and intra-actions between BSA and PAA in the self-assembly process, the nanoparticles and their components were measured by FT-IR method. The results are presented in Figure 6.

As for pure PAA, the characteristic bands of the stretching vibration of —OH group and carbonyl group as well as symmetry stretching vibration of carboxylic ion locate at around 3430, 1710, and 1413 cm^{-1}, respectively.[39,40] While for pure BAS, the characteristic bands of the stretching vibrations of —NH^- and carbonyl group as well as —NH(‖) of RC═O—NHR lie around 3417, 1644, and 1545 cm^{-1}, respectively. In the FT-IR spectrum of BAS/PAA nanoparticles at pH = 2.6, the stretching vibration bands of —NH^- and hydroxyl merged to one band at around 3432 cm^{-1}. Meanwhile, compared with pure PAA, the stretching vibration band of carbonyl group in PAA of BSA/PAA nanoparticle shifts to a higher wavenumber, 1718 cm^{-1}, and the stretching vibration band of amide carbonyl in BSA does not change in the nanoparticle compared with pure BSA, which indicates the interactions between BSA and PAA increase and hydrogen bonds interactions between amide groups and carboxyl groups exist at this pH.[41,42]

The Morphology of BSA/PAA Nanoparticles

AFM imaging provides evidence for the morphology of the obtained nanoparticles, as seen in Figure 7(a). In height image, the BSA/PAA nanoparticles appear as the intact spheres with an

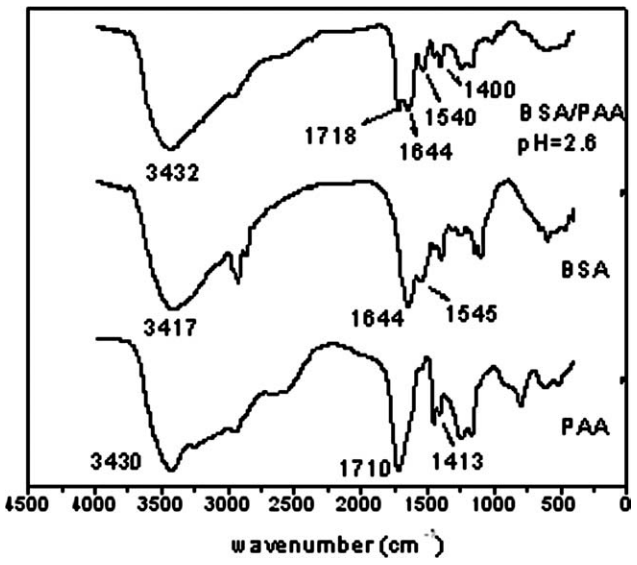

Figure 6. FTIR spectra of BSA, PAA, and BSA/PAA nanoparticles (BSA/PAA = 4.0, [BSA] = 1 mg/mL, pH = 2.6).

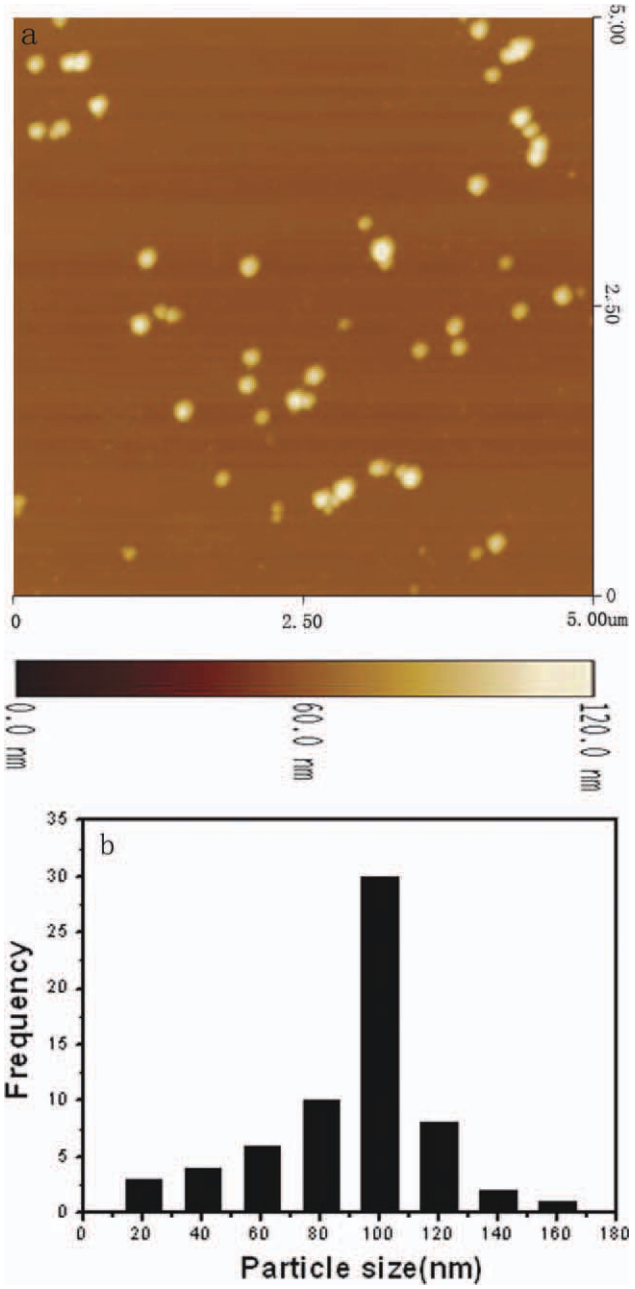

Figure 7. AFM image of BSA/PAA nanoparticles at pH = 2.6, (a) corresponding particle distribution (b) (BSA/PAA = 4.0, [BSA] = 1 mg/mL). [Color figure can be viewed in the online issue, which is available at wileyonlinelibrary.com.]

average diameter of 68.2 nm and an average height of 12.3 nm, while in phase image of Figure 7(a), the phase interface is observed. The bright regions in phase image correspond to hard part and the dark regions correspond to soft part. Apparently, the bigger sphere is loose. Some light point can be scanned in the little sphere for the compacted structure of nanoparticles. The distribution of the morphology of nanoparticles, including loose and compacted ones, is widely due to the polymerization method. A bar graph with number of particles versus given size range was also been researched according to Figure 7(a), as seen

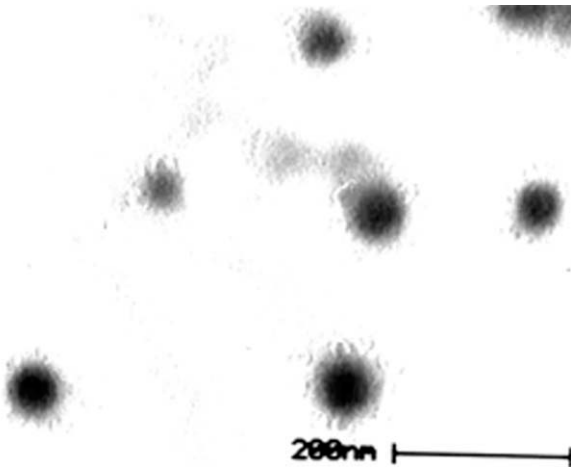

Figure 8. TEM image of BSA/PAA nanoparticles (BSA/PAA = 4.0, [BSA] = 1 mg/mL, pH = 2.6).

in Figure 7(b). The results show that about 50% nanoparticles distribute in the range between 80 and 100 nm, which means homogeneous distribution of the nanoparticles was achieved.

TEM was a powerful tool for observing the internal structure of polymeric assemblies. The morphology of BSA/PAA nanoparticles prepared at the weight ratio BSA/PAA = 4 at pH = 2.6 was observed by TEM. As displayed in Figure 8, nanoparticles show slightly deformed round contours. Furthermore, the core-shell structure of the particles was disclosed, although the contrast between the core and shell was fairly weak. BSA chains are supposed to be partly trapped in the nanoparticles core after interaction with PAA because of the electrostatic attractions at higher pH value and H-bonding interactions at pH lower than 2.5, while the rest of the BSA chains should form the shell of the nanoparticles. The resultant nanoparticles have cores composed of insoluble BSA/PAA inter-polymer complexes and shells of soluble BSA, and their structures were further locked by selectively cross-linking amide groups in BSA with glutaraldehyde. The average size of the particles is 83 nm.

CONCLUSIONS

Nano-scaled BSA/PAA particles were produced by noncovalent bonds induced self-assembly at acid pH area. ξ potential of BSA/PAA nanoparticles reaches the maximum around pH 2.5 and minimum at pH 4.0. At pH $>$ 4.0, the nanoparticles cannot exist stably. The suitable self-assembly pH for BSA/PAA nanoparticles is around pH 2.4−3.1 and the appropriate BSA/ PAA weight ratio for preparation is 3 $\sim$ 8. BSA chains are supposed to be partly trapped in the nanoparticles core after interaction with PAA because of the electrostatic attractions at higher pH value and H-bonding interactions at pH lower than 2.5, while the rest of the BSA chains should form the shell of the nanoparticles.

ACKNOWLEDGMENTS

This work was supported by the Program of Introducing Talents of Discipline to Universities (No. 111-2-04).

REFERENCES

1. Decher, G. *Science* **1997,** *277*, 1232.
2. Schna Dckel, A.; Hiller, S.; Reibetanz, U. *Soft Matter* **2007,** *3*, 200.
3. Hamlin, R. E.; Dayton, T. L.; Johnson, L. E. *Langmuir* **2007,** *23*, 4432.
4. Jewell, C. M.; Fuchs, S. M.; Flessner, R. M.; Raines, R. T.; Lynn, D. M. *Biomacromolecules* **2007,** *8*, 857.
5. Tang, Z. Y.; Wang, Y.; Podsiadlo, P. *Adv. Mater.* **2006,** *18*, 3203.
6. Muguruma, H.; Kase, Y. *Biosens. Bioelectron.* **2006,** *22*, 737.
7. Mohammed, J. S.; DeCoster, M. A.; McShane, M. J. *Langmuir* **2006,** *22*, 2738.
8. Michel, M.; Arntz, Y.; Fleith, G. *Langmuir* **2006,** *22*, 2358.
9. Jomaa, H. W.; Schlenoff, J. B. *Macromolecules* **2005,** *38*, 8473.
10. Ai, H.; Pink, J.; Shuai, X. T.; Boothman, D.; Gao, J. J. *Biomed. Mater. Res. A* **2005,** *73A*, 303.
11. Jewell, C. M.; Fuchs, S. M.; Flessner, R. M. *Biomacromolecules* **2007,** *8*, 857.
12. Muller, M.; Kessler, B.; Houbenov, N. *Biomacromolecules* **2006,** *7*, 1285.
13. Zezin, A.; Rogacheva, V.; Skobeleva, V. *Polym. Advan. Technol.* **2002,** *13*, 919.
14. Anatoly, F.; Myroslava, D.; Zeynep, M.; Yoshihito, O.; Mamed, M. *Biomacromolecules* **2001,** *2*, 270.
15. Mustafaev, M. I.; Yiicelztiirk, F.; Qrakoglu, B.; Bermek, E. J. *Immunol. Method.* **1996,** *197*, 31.
16. Babakhin, A. A.; DuBuske, L. M.; Wheeler, A. W. *Allergy Proc.* **1995,** *16*, 261.
17. Petrov, R. V.; Mustafaev, M. I.; Norimov, A. S. *Dokl Akad Nauk SSSR* **1990,** *312*, 505.
18. Petrov, R. V.; Khaitov, R. M.; Ignatov, P. I. *Zh Mikrobiol. Epidemiol. Immunobiol.* **1988,** *7*, 39.
19. Yajuan, L.; Xiaoyong, W.; Yilin, W. J. *Phys. Chem. B* **2006,** *110*, 8499.
20. Domurado, D.; Moreau, T.; Chotard-Ghodsnia, R. *Biomed. Polym. Polym. Therap.* **2001,** *12*, 159.
21. Panaitescu, L.; Ottenbrite, R. M. *J. Bioact. Compat. Polym.* **2002,** *17*, 357.
22. Petrov, R. V.; Mustafaev, M. I.; Norimov, A. S. *Biomed. Sci.* **1990,** *1*, 531.
23. Lechevalier, V.; Croguennec, T.; Pezennec, S.; Guérin-Dubiard, C.; Pasco, M.; Nau, F. *J. Agr. Food Chem.* **2003,** *51*, 6354.
24. Wu, D.; Xu, G.; Sun, Y.; Zhang, H.; Mao, H.; Feng, Y. *Biomacromolecules* **2007,** *8*, 708.
25. Ding, Y. H.; Shu, Y.; Ge, L. L.; Guo, R. *Coll. Surf. A* **2007,** *298*, 163.
26. Burt, J. L.; Gutierrez-Wing, C.; Miki-Yoshida, M.; José-Yacamán, M. *Langmuir* **2004,** *20*, 11778.
27. Mamed, M.; Seval, B.; Erhan, E. A.; Yılmaz, E.; Nesrin, A. *Radi. Phys. Chem.* **2001,** *60*, 567.

28. Mustsfsev, M.; Cirakoglu, A.; Sarac, S.; Ozturk, S.; Yucel, K.; Bermek, E. J. *Appl. Polym. Sci.* **1996,** *62*, 99.
29. Zhang, Y. W.; Jiang, M. *Acta Polym. Sin.* **2005,** *5*, 650.
30. Morawetz, H.; Hughes, W. L. *J. Phys. Chem.* **1952,** *56*, 64.
31. Mustafaev, M.; Osada, Y.; Matsukata, M.; Basalp, A.; Cüirakoglu, B.; Bermek, E. *Polym. Gels Networks* **1996,** *4*, 363.
32. Mustafaev, M.; Mustafaeva, Z.; Bermek, E.; Osada, Y. J. *Bioact. Compet. Polym.* **1998,** *13*, 33.
33. Malik, D. K.; Baboota, S.; Ahuja, A.; Hasan, S.; Ali, J. *Curr. Drug Deliv.* **2007,** *4*, 141.
34. Mercer, I. E.; Thomas, A. S. Concise Encyclopedia Biochemistry and Molecular Biology; de Gruyter: Berlin, **1997;** p 22−32.
35. Chen, Y.; Zheng, X. C.; Qian, H. Q.; Mao, Z. Q.; Ding, D.; Jiang, X. Q. *ACS Appl. Mater. Interf.* **2010,** *2*, 3532.
36. Wang, R. M.; Li, G.; Zhang, H. F.; He, Y. F.; He, N. P.; Lei, Z. Q. *Polym. Advan. Technol.* **2010,** *21*, 685.
37. Song, S. W.; Hidajat, K.; Kawi, S. *Chem. Commun.* **2007,** 4396.
38. Goodman, D. S.J. *Am. Chem. Soc.* **1958,** *80*, 3892.
39. Gonzalez, B. C.; Rodriguez, L. J.; Velasquez, M. M. *Langmuir* **1997,** *13*, 1938.
40. Zhao, J.; Allen, C.; Eisenberg, A. *Macromolecules* **1997,** *30*, 7143.
41. Yu, Y. S.; Eisenberg, A. J. *Am. Chem. Soc.* **1997,** *119*, 8383.
42. Jiang, H. L.; Zhu, K. J. *J. Appl. Polym. Sci.* **2001,** *80*, 1416.